Structure-based classification of 45 FK506-binding proteins

J. A. Somarelli,[1] S. Y. Lee,[2] J. Skolnick,[2] and R. J. Herrera[1]*

[1] Department of Biological Sciences, OE304, Florida International University, Miami, Florida 33199

[2] Center for the Study of Systems Biology, School of Biology, Georgia Institute of Technology, Atlanta, Georgia 30332

ABSTRACT

The FK506-binding proteins (FKBPs) are a unique group of chaperones found in a wide variety of organisms. They perform a number of cellular functions including protein folding, regulation of cytokines, transport of steroid receptor complexes, nucleic acid binding, histone assembly, and modulation of apoptosis. These functions are mediated by specific domains that adopt distinct tertiary conformations. Using the Threading/ASSEmbly/Refinement (TASSER) approach, tertiary structures were predicted for a total of 45 FKBPs in 23 species. These models were compared with previously characterized FKBP solution structures and the predicted structures were employed to identify groups of homologous proteins. The resulting classification may be utilized to infer functional roles of newly discovered FKBPs. The three-dimensional conformations revealed that this family may have undergone several modifications throughout evolution, including loss of N- and C-terminal regions, duplication of FKBP domains as well as insertions of entire functional motifs. Docking simulations suggest that additional sequence segments outside FKBP domains may modulate the binding affinity of FKBPs to immunosuppressive drugs. The docking models also indicate the presence of a helix-loop-helix (HLH) region within a subset of FKBPs, which may be responsible for the interaction between this group of proteins and nucleic acids.

INTRODUCTION

Immunophilins are a diverse family of chaperones found throughout all known taxonomic groups. These proteins are also known as peptidyl-prolyl *cis-trans* isomerases (PPIases) for their ability to convert proline bonds from *cis* to *trans* form, a rate-limiting step in protein folding.[1–6] In addition, immunophilins can be divided into two subfamilies based on their ability to bind specific immunosuppressive drugs. Those that bind cyclosporin are known as cyclophilins while those that associate with FK506, FK1706, rapamycin, and other derivatives are known as the FK506-binding proteins (FKBPs).

In humans, 15 FKBPs have been identified thus far.[7] The smallest and most comprehensively studied of these is FKBP1 (also known as FKBP12), which is 108 amino acids in length (12 kDa) and contains just one FKBP domain. Other FKBPs possess up to four FKBP domains along with several additional functional motifs, including nucleic acid binding regions,[8] tetratricopeptide repeat (TPR) motifs,[6] Ef-hand (EfH) calcium-binding domains,[9] as well as transmembrane,[7] nuclear localization[8,10] and endoplasmic reticulum (ER) signal sequences.[11]

FKBPs from numerous other organisms also possess variable numbers and types of domains, which enable this protein family to perform a wide variety of cellular functions in addition to protein folding. For example, in mammals, the FK506-FKBP1 complex binds to and inhibits calcineurin, a serine-threonine phosphatase and activator of NFAT (nuclear factors of activated T-cells).[3,12] The NFAT group of transcription factors regulates production of a number of T-cell specific activators, including cytokines IL-2 and IL-5, as well as cell surface receptors and signaling proteins.[13,14] FKBP1 also mediates intracellular calcium release through its interaction with the ryanodine receptors (RyR) in skeletal and cardiac muscle[15,16] (and included references).

In addition, FKBP3 (FKBP25) from humans, FKBP46 from *Spodoptera frugiperda* (fall army worm), FKBP45 from *Bombyx mori* (silk moth), FKBP39 in *Drosophila melanogaster*, FKBP3 in *Saccharomyces cerevisiae* and others (Table I) possess signals for nuclear localization as well as nucleic

Table I
FKBPs used in TASSER Predictions

Accession no.[a]	Species[b]	Protein	Sequence identity[c]	Template[d]	C-score[e]
P54397	Dm	FKBP39	30.3% (201/357)	1fd9	−0.737
A			19.2% (104/135)	1xo9	−2.058
B			29.4% (201/222)	1fd9	0.730
NP_524895	Dm	FKBP59	44.4% (351/439)	1kt0	1.021
P48375	Dm	FKBP1	39.0% (105/108)	1fd9	3.330
AAF16717	Ms	FKBP	36.2% (105/108)	1fd9	3.350
AAY86706	Bm	FKBP45	30.6% (193/402)	1fd9	−2.562
A			21.6% (190/205)	1u00	−3.190
B			30.7% (192/197)	1fd9	1.175
Q26486	Sf	FKBP46	27.7% (191/412)	1fd9	−2.444
A			18.6% (188/218)	1kt0	−3.366
B			27.9% (190/194)	1fd9	0.988
EAL41402	Ag	FKBP	45.3% (349/396)	1kt0	2.117
EAA06906	Ag	FKBP	25.9% (263/318)	1kt0	1.128
EAA08436	Ag	FKBP	34.1% (132/137)	1fd9	2.876
EAA10152	Ag	FKBP	44.6% (130/211)	1jvw	−0.665
EAA44266	Ag	FKBP	24.5% (323/405)	1kt0	−0.017
A			14.9% (67/67)	1e32	−0.764
B			38.2% (55/55)	2awg	1.044
C			26.9% (208/283)	1kt0	−0.603
EAA00094	Ag	FKBP	23.9% (272/325)	1kt0	1.510
EAA00155	Ag	FKBP	40.0% (105/108)	1fd9	3.340
XP_972491	Tc	FKBP39	30.4% (191/349)	1fd9	−2.084
A			19.0% (216/233)	1kt0	−3.777
B			37.2% (113/116)	1fd9	3.075
BAD90849	Bm	FKBP59	47.2% (356/451)	1kt0	1.055
P62942	Hs	FKBP1	36.2% (105/108)	1fd9	3.282
AAH91475	Hs	FKBP2	30.5% (128/142)	1fd9	2.664
NP_002004	Hs	FKBP3	29.0% (200/224)	1fd9	2.119
Q02790	Hs	FKBP4	60.3% (353/459)	1kt0	0.747
AAI11051	Hs	FKBP5	98.0% (353/457)	1kt0	0.821
A			28.5% (137/157)	1fd9	1.711
B			99.1% (117/117)	1kt0	1.281
C			28.1% (135/183)	1ihg	0.435
O75344	Hs	FKBP6	31.1% (254/327)	1kt0	1.077
Q9Y680	Hs	FKBP7	32.3% (127/259)	2f4e	−0.516
NP_036313	Hs	FKBP8	24.8% (330/413)	1kt0	0.024
NP_0090210	Hs	FKBP9	26.3% (346/570)	1kt0	−0.932
			21.1% (261/269)	1kt0	1.501
			31.3% (115/119)	1jvw	2.032
			36.0% (89/182)	1a7x	−0.609
NP_068758	Hs	FKBP10	27.1% (277/582)	1kt0	−2.058
A			30.0% (207/280)	1kt0	−0.349
B			25.8% (244/264)	1kt0	0.820
C			21.1% (38/38)	1kt0	0.588
Q9NYL4	Hs	FKBP11	32.5% (120/201)	1fd9	0.590
NP_060416	Hs	FKBP14	34.3% (143/211)	1jvw	−0.155
P38911	Sc	FKBP	23.9% (201/411)	1fd9	−2.503
A			17.6% (204/209)	1fgg	−3.059
B			24.0% (200/202)	1fd9	0.842
Q6CWE8	Kl	FKBP	29.5% (193/418)	1fd9	−2.742
A			19.5% (215/223)	1zjc	−1.960
B			29.0% (193/195)	1fd9	0.861
EAL64753	Dd	FKBP	32.5% (197/364)	1fd9	−1.398
A			25.2% (123/158)	1xo9	−2.275
B			32.7% (196/206)	1fd9	0.775
CAB81345	At	FKBP	29.5% (190/487)	1fd9	−2.418
A			20.3% (256/291)	1kt0	−3.205
B			29.6% (189/196)	1fd9	1.148
NP957178	Dr	FKBP8	25.7% (342/406)	1kt0	0.691
A			19.4% (103/103)	1ign	−2.292
B			19.0% (105/115)	1kt0	1.286
C			30.9% (136/188)	1ihg	0.387

(*Continued*)

Table I
Continued

Accession no.[a]	Species[b]	Protein	Sequence identity[c]	Template[d]	C-score[e]
AAB05213	Sm	FKBP	36.3% (336/430)	1kt0	0.380
A			30.1% (133/152)	1fd9	1.375
B			21.7% (106/109)	1kt0	0.044
C			33.1% (136/169)	1kt0	0.266
AAQ84562	Mm	FKBP8	22.8% (337/402)	1kt0	−0.035
A			26.3% (95/103)	1ign	−1.834
B			18.6% (97/114)	1kt0	1.132
C			27.2% (136/185)	1ihg	0.127
NP_001032257	Rn	FKBP8	24.2% (335/403)	1kt0	0.036
A			25.8% (97/104)	1ign	−1.785
B			20.0% (95/114)	1kt0	1.139
C			27.9% (136/185)	1ihg	0.304
AAF08340	Br.m	FKBP	25.4% (142/164)	1jvw	2.441
AAD01596	Ov	FKBP	35.8% (134/137)	1jvw	2.598
AAD01595	Br.m	FKBP	35.7% (115/137)	1fd9	2.493
AAD01594	Di	FKBP	30.5% (131/137)	1fd9	2.653
CAA53594	Bs	FKBP	33.9% (115/134)	1fd9	2.677
AAB65470	Ce	FKBP	29.3% (188/261)	1fd9	−0.181
A			9.4% (53/56)	1ugj	−0.204
B			28.9% (187/205)	1fd9	1.068
AAD01597	Br.m	FKBP	42.8% (353/426)	1kt0	1.749
NP_417806	Ec	FKBP	37.1% (202/270)	1fd9	1.169
A64403	Mj	FKBP	44.7% (150/240)	1ix5	−0.241
A			45.0% (149/158)	1ix5	1.628
B			20.7% (82/82)	1ogc	−0.424
XP_713635	Ca	FKBP	25.4% (189/426)	1fd9	−2.579
A			17.0% (224/235)	1p35	−2.047
B			25.6% (180/191)	1fd9	0.871

C-score = ln $((M/R \times M_{tot}) \times Z)$, where M represents the multiplicity of structures in a SPICKER cluster, M_{tot} is the total number of structures submitted for clustering and R is the average relative mean standard deviation (RMSD) of the structures relative to the cluster centroid. Predictions with low C-scores indicate that the foldable fraction is low and models become more unreliable.
Highlighted rows indicate that empirically determined structures are available in the PDB.
[a]Genbank accession numbers for all FKBPs used in the TASSER predictions are listed. For proteins with C-scores below 0, the structure was divided into A, B and C domains, as described in[e].
[b]Species include: Dm (*Drosophila melanogaster*), Ms (*Manduca sexta*), Bm (*Bombyx mori*), Sf (*Spodoptera frugiperda*), Ag (*Anopheles gambiae*), Tc (*Tribolium castaneum*), Hs (*Homo sapiens*), Sc (*Saccharomyces cerevisiae*), Kl (*Kluyveromyces lactis*), Dd (*Dictyostelium discoideum*), At (*Arabidopsis thaliana*), Dr (*Danio rerio*), Sm (*Schistosoma mansoni*), Mm (*Mus musculus*), Rn (*Rattus norvegicus*), Br.m (*Brugia malayi*), Ov (*Onchocerca volvulus*), Di (*Dirofilaria immitis*), Bs (*Botryllus schlosseri*), Ce (*Caenorhabditis elegans*), Ec (*Escherichia coli*), Mj (*Methanococcus jannaschii*), Ca (*Candida albicans*).
[c]Sequence identity is calculated between the top 1 template and the target sequence, listed here as a percentage. The coverage is indicated in parentheses as the number of residues from the top 1 template over the number of residues in each target sequence.
[d]The PDB ID is listed for each template used in the predictions.
[e]The C-score is the confidence score used to evaluate the certainty of the TASSER structure prediction.

acid binding domains and may play a role in nucleosome assembly and/or pre-mRNA splicing.[8,17–19]

A different group of FKBPs containing TPR (tetratricopeptide repeat) domains are involved in transport of a number of high molecular weight complexes, including transient receptor potential-like (TRPL) proteins in insects[20] and high-affinity steroid receptor complexes in both plants and vertebrates.[21,22] For example, FKBP4s and FKBP5s promote and inhibit the formation of glucocorticoid receptor (GR) and progesterone receptor (PR) complexes, respectively.[23] FKBP8 (FKBP38) orthologues contain an N-terminal FKBP domain and a single TPR motif. These proteins regulate apoptosis via formation of an active Ca^{2+}/calmodulin (CaM)/Bcl-2 complex.[24–26] Subsequent to binding Ca^{2+} and CaM, FKBP8 undergoes conformational changes, which enables the complex to interact with and sequester Bcl-2 from the mitochondria, thus promoting cell death.[26]

In humans, FKBP2, 7, 9, 10, 11, and 14 possess variable numbers of FKBP domains and are associated with the endoplasmic reticulum (ER). Unlike the other ER localized proteins in this family, FKBP7, FKBP9, and FKBP10 contain Ca^{2+} binding Ef-H regions. In spite of these differences, it is likely that all of these proteins have similar functions as mediators of protein folding and secretion.[7]

Despite the rather large body of work surrounding the functional characterization of FKBPs in several organisms, relatively few tertiary structures exist for this protein family. Most of the crystallographic and/or NMR data regarding FKBPs on the Protein Data Bank (PDB) concerns FKBP1 and its interactions with various small molecules including the immunosuppressants FK506,[27]

rapamycin,[27,28] FK1012[29] as well as other ligands. Comparison of FKBP1 in association with 16 distinct ligands suggests that different conformational changes are involved with each complex.[27] Aside from FKBP1 (PDB ID: 1FKK), three-dimensional configurations are available for a limited number of other FKBPs, including one each from *Methanococcus thermolithotrophicus* (PDB ID: 1IX5), *Escherichia coli* (PDB ID: 1Q6U), and *Caenorhabditis elegans* (PDB ID: 1R9H), two from *Arabidopsis thaliana* (PDB ID: 2IF4 and 1U79), as well as for FKBP4 (PDB ID: 1N1A) and FKBP5 (PDB ID: 1KT0) from humans. Wu et al.[30] found that differences in both the orientations and sequences of FKBP4 and FKBP5 may be responsible for the distinct cellular roles of these proteins. In addition, individual FKBP domains from FKBP3 (PDB ID: 1PBK) and FKBP8 (PDB ID: 2F2D and 2AWG) are also available.

Utilizing the protein tertiary structure prediction algorithm TASSER,[31] tertiary structures were predicted for 45 FKBPs in 23 species. Generating three-dimensional models for a comprehensive number of FKBPs provides information on the structure–function relationships as well as the different functional roles adopted by FKBPs throughout evolution. Some of the structures represent a first approximation of several uncharacterized domains within specific FKBPs. The predicted structures also revealed significant similarity at the level of tertiary conformations among groups of orthologous FKBPs, alluding to gene duplications and domain insertion events early in evolution. Docking simulations suggest that additional incorporation of domains may reduce the affinity of FKBP domains for FK506 and/or create novel active sites for drug binding, possibly by altering the steric hindrance surrounding the active site.

MATERIALS AND METHODS

Selection of FKBP sequences for tertiary structure analyses

Amino acid sequences from a total of 45 FKBPs were obtained from the National Center for Bioinformatics (NCBI) database (http://www.ncbi.nlm.nih.gov/) and examined with the PROSPECTOR_3 algorithms, an iterative threading program that combines both close and distant sequence alignments as well as secondary structure predictions to create a subset of targets for use in subsequent identification of pair interactions.[32] To understand the complexity of folding patterns within the entire FKBP family, sequences were chosen representing a range of sizes and domains found within these proteins. Genbank accession numbers for all sequences are listed in Table I. Traditionally, FKBPs have been classified according to molecular weight (e.g. FKBP45, 45 referring to 45 kDa). Yet, in humans a different set of designations has been adopted. In this article, FKBP groups are referred to based on the human FKBP nomenclature (i.e., FKBP1-14).

When we make reference to specific proteins in other organisms, we use names based on molecular weight (i.e., FKBP39 in *Drosophila melanogaster*). To assess the accuracy of our predictions, three FKBP sequences with complete tertiary structures from empirically determined data were included (highlighted in gray in Table I).

Prediction of FKBP tertiary structures

All FKBP folding patterns were predicted using the TASSER methodology as previously described.[31] Briefly, TASSER utilizes the PROSPECTOR_3 threading algorithms to identify empirically determined protein templates,[32] followed by tertiary structure assembly using Monte Carlo sampling and clustering with the program SPICKER.[33] This data set was further refined by generating a set of consensus contacts for each of four threading iterations. Finally, sets of predicted side chain contacts, continuous local fragments and folding templates were constructed. The conditions and parameters for this group of programs were based on a template library consisting of 3575 representative structures obtained from the PDB (http://www.pdb.org) and clustered into representative structural families.

Parallel hyperbolic Monte Carlo sampling (PHS) was utilized to position the continuous aligned protein segments and assemble a full protein model from the threading templates. A total of 40 replicas were generated by PHS and the 14 low-temperature replica trajectories were clustered by SPICKER, from which the five highest structural density clusters were selected.[33] The top model for each FKBP was employed in all subsequent steps described below.

A confidence score (C-score) was also generated to evaluate the certainty of the TASSER predictions: C-score $= \ln((M/R \times M_{tot}) \times Z)$, where M represents the multiplicity of structures in a SPICKER cluster, M_{tot} is the total number of structures submitted for clustering and R is the average relative mean standard deviation (RMSD) of the structures relative to the cluster centroid (Table I). Predictions with negative C-scores are more unreliable, while those with positive C-scores are more likely to represent authentic native protein conformations.[34] For cases in which the C-score was below 0, the protein was divided into multiple segments (labeled A, B, and C in Table I) and TASSER was rerun for each domain. This provides for greater reliability for specific domains within a protein and identifies regions of low certainty. All 45 predicted structures are available on the Proteins: Structure, Function and Bioinformatics website (Online Supplementary File 1).

Alignment and superposition of predicted structures

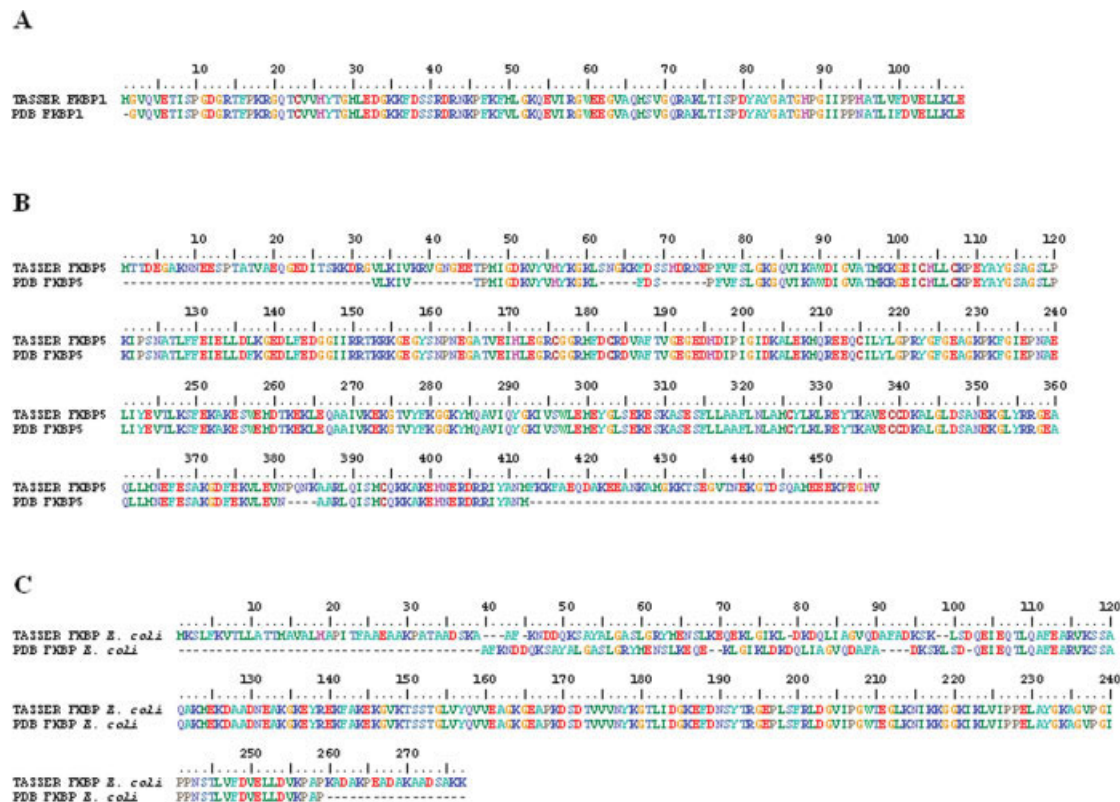Conformational differences among FKBPs were compared by alignment and superposition using the Java-based

Figure 1

FKBP models closely represent previously determined crystal structures. Pairwise structural alignments using ClustalW_3D between empirically generated protein structures and in silico derived models revealed that the TASSER set of programs creates complete protein representations that match closely the known crystal structures. TASSER models are on the top, with the PDB structures at the bottom of each pair. The numbered bar at the top indicates position of amino acids. (A) TASSER generated model of FKBP1 from H. sapiens matches exactly to that of its corresponding conformation in the PDB (PDB ID: 1FKK), with the exception of a single methionine in the PDB structure. (B) Both N- and C-terminal regions of FKBP5 from H. sapiens are missing in the crystallograph (dashes) compared to the TASSER model. The structural alignment delineates four additional internal regions that are incomplete in the PDB conformation. (C) Although the N- and C-termini of the E. coli FKBP from TASSER is more complete, the first 102 amino acids are shifted by 1 to 4 positions compared to the PDB structure. [Color figure can be viewed in the online issue, which is available at www.interscience.wiley.com.]

STRAP program available at: http://www.charite.de/bioinf/strap/.[35] Structure predictions were aligned and superimposed using ClustalW_3D and Superimpose3D_CE, respectively, within STRAP. FKBPs were divided into groups based on (1) their molecular weight, (2) the number and type of motifs within each protein and (3) their predicted tertiary structures.

Docking simulations

A three-dimensional model of FK506 was extracted from a solution structure of the FKBP1-FK506 complex (PDB ID: 1FKF). A three-dimensional model of a stem-loop (hair-pin structure) RNA was obtained from a U1A protein-RNA complex (PDB ID: 1AUD). FK506 or stem-loop (hair-pin structure) RNA was input as the ligand into the ZDOCK server (http://zdock.bu.edu/), with each FKBP structure input as the receptor. No residues were selected to either force into or block from the active site. Ligand/re-ceptor complexes were generated using the Create Complexes Java script (http://zdock. bu.edu/cgi/help.cgi).

Prediction of molecular weight and pI

The theoretical molecular weight and isoelectric point (pI) were calculated for each FKBP sequence using the Compute pI/MW tool available on the Expert Protein Analysis System (ExPASy) proteomics server (http://ca.expasy.org/tools/pi_tool.html).[36,37]

RESULTS

Generation of three-dimensional models and comparison with crystal structures

The amino acid sequences of 45 FKBPs among 23 species representing the five taxonomic kingdoms, including Archaea, Bacteria, Fungi, Plantae, and Animalia were
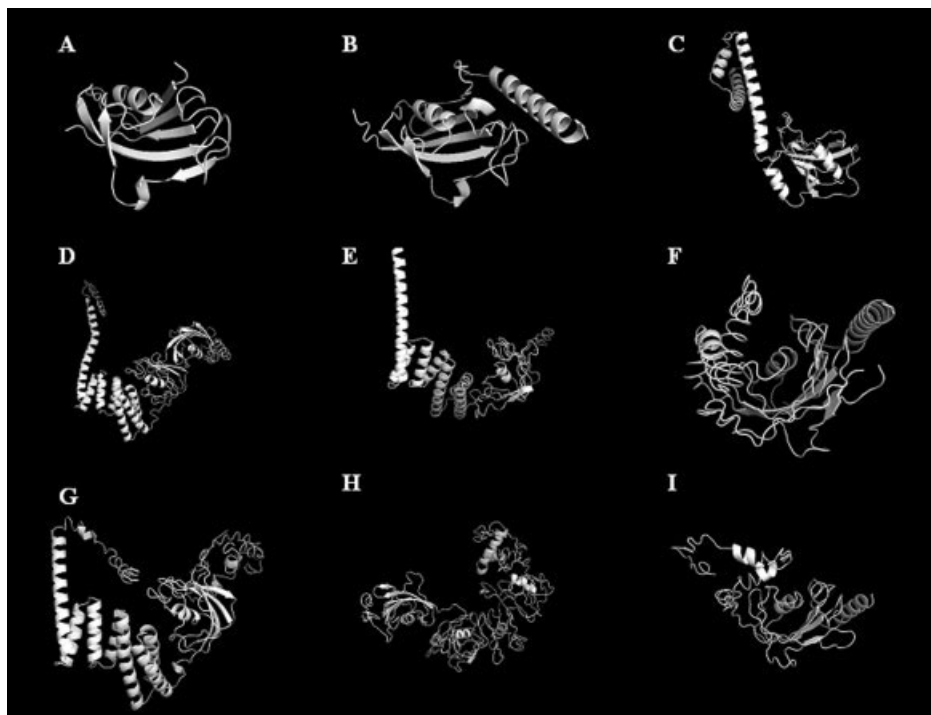
Figure 2

FKBP tertiary structures. Tertiary structures were predicted using the TASSER set of programs and assembled into groups of potential homologues. Models were rendered using the PyMol viewer within STRAP. Figures (A) through (I) correspond to Homo sapiens *FKBP1, FKBP2, FKBP3, FKBP4/5, FKBP6, FKBP7, FKBP8, FKBP9/10 and FKBP11/14, respectively. FKBPs from other organisms were placed into groups of orthologues based on structural similarity to one or more of the* Homo sapiens *FKBPs.*

selected from the NCBI protein database. Complete, empirically determined solution structures are available on the PDB for three of the 45 proteins, including one from *Escherichia coli* (PDB ID: 1Q6U) and two from

Homo sapiens (FKBP1 with PDB ID: 1FKK and FKBP5 with PDB ID: 1KT0) (highlighted in gray in Table I). These were utilized as comparative controls in the TASSER predictions. Solution structures are also available
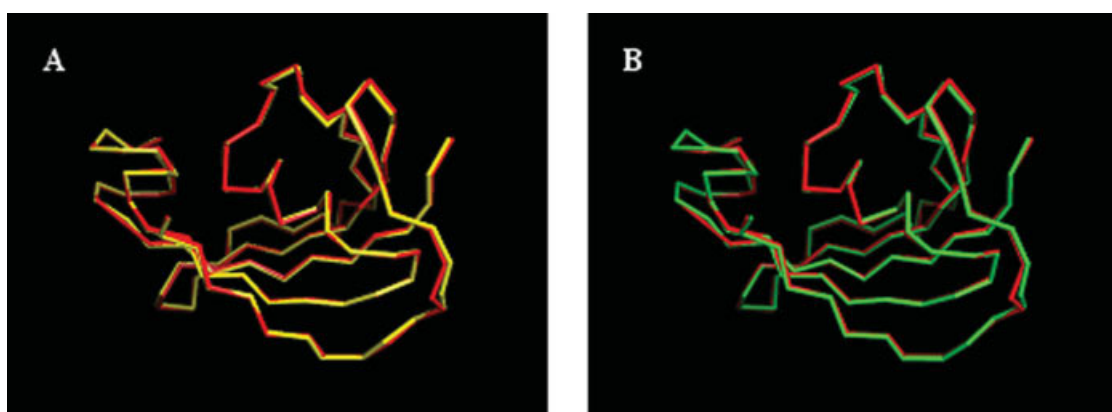

Figure 3

Superposition of Homo sapiens *FKBP1 with insect homologues. Putative orthologues were superimposed in a pairwise fashion using the STRAP program to assess the degree of structural similarity among groups of FKBPs. FKBP1 from* Homo sapiens *(red) is superimposed with FKBPs from (**A**)* Anopheles gambiae *(yellow) and (**B**)* Manduca sexta *(green). Although FKBPs exist in all known organisms, their cellular roles have not been identified in a number of taxonomic groups. Structural similarity suggests that functional parallelisms may exist in a variety of organisms and the superpositions enable us to hypothesize about the utility of the FKBPs in species for which no function has been characterized.*

for the N- and C-terminal domains of FKBP4 (PDB ID: 1Q1C and 1QZ2), as well as the FKBP domain of FKBP8 (PDB IDs: 2F2D and 2AWG) in humans.

To understand how well our best models fit the known folding properties of FKBPs, both empirically-determined and predicted FKBPs were superimposed using the Superimpose_CE program within the Java-based STRAP software.[35] With few exceptions, the predicted structures were nearly identical to their empirically generated counterparts (Online Supplementary File 2). Furthermore, the predicted structure of FKBP5 from humans is more complete than the human FKBP5 crystallographic structure of Sinars et al.,[22] with additional residues at the N- and C- termini (Met[1]-Val[33] and Met[413]-Ala[459], respectively). Similarly, the *Escherichia coli* FKBP model contains additional amino acids at the N- and C- termini when compared with its counterpart in the PDB (Met[1]-Ala[39] and Lys[253]-Lys[270], respectively). Pair-wise structural alignments between TASSER generated models and complete FKBPs from the PDB further demonstrate the high degree of similarity between simulated and empirically determined conformations (see Fig. 1).

Assignment of FKBPs into groups

Overall sequence identity between FKBP models and PDB templates ranges from 9.4 to 99.1%, with an average identity of 30.8%. Overall coverage of PDB templates to predicted FKBP targets ranges from 44.4 to 100% with an average of 81.8%. A total of 44% (20/45) of predicted structures had negative *C*-scores in one or more domains; yet, comparisons with empirically determined conformations and the assembly of FKBPs into groups of orthologues allowed inferences to be made regarding the overall structure and function of many of these proteins. The creation of these groups may provide information regarding the potential function of newly discovered FKBPs.

The 45 FKBPs were subdivided into six major groups, based on their size and structural characteristics (Table II). Using the STRAP program, best models for members of each group were superimposed in a pair-wise fashion to understand subtle differences within the tertiary conformations of FKBP orthologues. The first group of proteins consists of FKBP1 orthologues. These proteins are made up of a single FKBP domain. Figure 2(A) illustrates the human FKBP1 (PDB ID: 1FKK) tertiary structure.

In comparison with FKBP1, proteins in the second group possess one FKBP domain, as well as an additional N-terminal alpha helix and extra C-terminal amino acids. This group of proteins includes orthologues to human FKBP2 [Fig. 2(B)]. The N-terminal helix contains a signal peptide responsible for membrane association while the additional C-terminal amino acids are essential for ER localization.[11] Two FKBPs from *Brugia malayi* (GA no.: AAD01595 and AAF08340) as well as FKBPs from *Onchocerca volvulus* (GA no.: AAD01596), *Dirofilaria*

immitis (GA no.: AAD01594), *Botryllus schlosseri* (GA no.: CAA53594) and *Anopheles gambiae* (GA no.: EAA08436) closely fit the structure of FKBP2 (FKBP13) from humans. The archaeal FKBP from *Methanococcus jannaschii* also appears to be most closely related to this group despite several distinct differences. Particularly, the N-terminal signal sequence is missing and two loop structures protrude from the FKBP domain at Glu[34]-Tyr[50] and Lys[90]-Glu[142]. The *M. jannaschii* FKBP contains two additional small C-terminal helices at Asp[159]-Lys[240]. An empirically determined structure from *Methanococcus thermolithotrophicus* reveals a similar pattern, with an insertion of three alternating β sheets and a single, small α-helix extending from the FKBP domain[38] (Online Supplementary File 1). This FKBP, however, does not contain the C-terminal helix motif found in the *M. jannaschii* FKBP. FKBP11 and FKBP14 from humans [Fig. 2(I)] also possess this C-terminal helical structure and both are targeted for the ER[7]; however, the two loops within the *M. jannaschii* and *M. thermolithotrophicus* FKBP domains seem to have been lost in these two human orthologues as well as in all other members assigned to this group (Table II). Alternatively, these sequences may represent lineage-specific acquired characteristics incorporated subsequent to the separation from other taxa. FKBP14 appears to be more similar than FKBP11 to the *M. jannaschii* FKBP, with an 11 amino acid C-terminal helix-loop region that is lacking in FKBP11.

The FKBP3 (FKBP25) homologues comprise the third group, which contain just one C-terminal FKBP domain, a central helix-loop-helix (HLH) motif, which is thought to bind nucleic acid,[8,17,19] and an N-terminal area of low structural complexity [Fig. 2(C)]. These proteins range in size from 224 to 487 amino acids and differ in their size and three-dimensional arrangement at the N-terminal low complexity region; however, the tertiary structure of both the central α-helix and the FKBP domain maintains a striking similarity among all proteins in this group. The smallest of these proteins, *Homo sapiens* FKBP3 and *Escherichia coli* FKBP, lack the low complexity N-terminal region.

The fourth group contains FKBP6 and FKBP8 orthologues, with a single C-terminal FKBP domain [Fig. 2(E)]. Although all of the members of this group possess a similar tertiary structure, the FKBP6s lack an N-terminal TPR motif (Table I). The fifth group is distinguished by the presence of an EfH domain in the C-termini and one to four FKBP domains at the N-termini [Fig. 2(F, G)]. The final group identified includes human FKBP4 and FKBP5 orthologues with two FKBP motifs and a single TPR region [Fig. 2(D)]. Another member of group 6, FKBP3 from *Caenorhabditis elegans*, is missing the TPR domain, and may represent a protein whose sequence has been incompletely characterized or became truncated at some point throughout evolution. Addition-

Table II
FKBP Orthologues Grouped by Structural and Physico-Chemical Characteristics

	Accession number	Protein	Species	FKBP domains	HLH domains	TPR domains	EfH domains	Predicted Size (kDa)	Predicted pI
Group 1	P48375	FKBP1	*Drosophila melanogaster*	1	—	—	—	11.7	7.85
	AAF16717	FKBP	*Manduca sexta*	1	—	—	—	11.8	7.86
	EAA00155	FKBP	*Anopheles gambiae*	1	—	—	—	11.6	7.90
	P62942	FKBP1	*Homo sapiens*	1	—	—	—	12.0	7.89
Group 2	A64403	FKBP	*Methanococcus jannaschii*	1	—	—	—	27.0	5.80
	AAD01596	FKBP	*Onchocerca volvulus*	1	—	—	—	15.4	5.46
	AAD01595	FKBP	*Brugia malayi*	1	—	—	—	15.3	5.86
	AAD01594	FKBP	*Dirofilaria immitis*	1	—	—	—	15.2	4.88
	CAA53594	FKBP	*Botryllus schlosseri*	1	—	—	—	14.8	7.64
	AAF08340	FKBP	*Brugia malayi*	1	—	—	—	18.0	5.92
	EAA08436	FKBP	*Anopheles gambiae*	1	—	—	—	15.1	7.74
	Q9NYL4	FKBP11	*Homo sapiens*	1	—	—	—	22.2	9.44
	NP_060416	FKBP14	*Homo sapiens*	1	—	—	—	24.2	5.70
	AAH91475	FKBP2	*Homo sapiens*	1	—	—	—	15.6	9.00
Group 3	NP_417806	FKBP	*Escherichia coli*	1	1	—	—	28.9	8.39
	EAL64753	FKBP	*Dictyostelium discoideum*	1	1	—	—	40.0	4.57
	P38911	FKBP	*Saccharomyces cerevisiae*	1	1	—	—	46.6	4.36
	Q6CWE8	FKBP	*Kluyveromyces lactis*	1	1	—	—	47.3	4.39
	XP_713635	FKBP	*Candida albicans*	1	1	—	—	47.7	4.33
	CAB81345	FKBP	*Arabidopsis thaliana*	1	1	—	—	53.3	4.91
	P54397	FKBP39	*Drosophila melanogaster*	1	1	—	—	39.3	4.69
	AAY86706	FKBP45	*Bombyx mori*	1	1	—	—	44.7	4.75
	Q26486	FKBP46	*Spodoptera frugiperda*	1	1	—	—	45.8	4.68
	XP_972491	FKBP39	*Tribolium castaneum*	1	1	—	—	38.9	4.79
	NP_002004	FKBP3	*Homo sapiens*	1	1	—	—	25.2	9.29
Group 4	EAA10152	FKBP	*Anopheles gambiae*	1	—	—	—	23.3	4.64
	EAA00094	FKBP	*Anopheles gambiae*	1	—	1	—	38.1	7.68
	EAA44266	FKBP	*Anopheles gambiae*	1	—	1	—	44.7	5.01
	EAA06906	FKBP	*Anopheles gambiae*	1	—	1	—	36.9	6.35
	NP_957178	FKBP8	*Danio rerio*	1	—	1	—	43.8	5.13
	NP_001032257	FKBP8	*Rattus norvegicus*	1	—	1	—	43.6	5.13
	AAQ84562	FKBP8	*Mus musculus*	1	—	1	—	43.5	5.08
	NP_036313	FKBP8	*Homo sapiens*	1	—	1	—	44.6	4.78
	O75344	FKBP6	*Homo sapiens*	1	—	—	—	37.2	6.48
Group 5	Q9Y680	FKBP7	*Homo sapiens*	1	—	—	1	30.0	6.09
	EAL24461	FKBP9	*Homo sapiens*	4	—	—	1	63.0	4.91
	NP_068758	FKBP10	*Homo sapiens*	4	—	—	1	64.3	5.36
Group 6	AAB65370	FKBP	*Caenorhabditis elegans*	2	—	—	—	29.0	5.30
	AAD01597	FKBP	*Brugia malayi*	2	—	1	—	47.5	5.76
	AAB05213	FKBP	*Schistosoma mansonii*	1	—	1	—	48.2	5.61
	NP_524895	FKBP59	*Drosophila melanogaster*	2	—	1	—	48.8	5.31
	EAL41402	FKBP	*Anopheles gambiae*	2	—	1	—	43.9	6.15
	BAD90849	FKBP59	*Bombyx mori*	2	—	1	—	51.0	8.00
	Q02790	FKBP4	*Homo sapiens*	2	—	1	—	51.2	5.71
	AAI11051	FKBP5	*Homo sapiens*	2	—	1	—	51.8	5.35

ally, based on sequence alignments, the *Schistosoma mansoni* FKBP in group four appears to have just one FKBP domain along with the TPR motif (data not shown); however, superposition of this protein model with other members of its group suggests that it maintains the same tertiary conformation as other FKBP4 or FKBP5 orthologues.

DISCUSSION

Evaluation of TASSER generated models

The tertiary structures three of the 45 FKBPs reported here (highlighted in gray in Table I) have been previously characterized by empirical techniques. To assess the accuracy of the TASSER predictions, the crystal structures of these FKBPs were compared to their corresponding TASSER models. Both structural alignments (see Fig. 1) and superpositions (Online Supplementary File 2) revealed significant overlap between PDB structures and TASSER conformations. In addition, the TASSER models all have positive C-scores. Although it is possible that some of the predicted configurations, in particular those with negative C-scores, do not represent biologically realistic conformations, these comparisons suggest that the *in silico* derived models may closely represent the native folding characteristics of these proteins.

Assembly of FKBP structures into groups

Using the TASSER threading methodology, an assembly of 45 FKBP tertiary structure predictions was created. Although the interactions of several FKBPs have been well documented, the cellular role(s) of FKBPs in a number of organisms remains to be elucidated. By utilizing a combination of functionally characterized structures as well as several empirically determined three-dimensional conformations, we were able to place FKBPs of unknown configuration into groups of potential homologues (Table I). This information should provide valuable insight into the structure–function relationships of this diverse group of proteins. Characteristics such as molecular weight, pI, and protein sequence can be highly variable within groups (Table II). However, the structure predictions are strikingly similar among the members of each group. For example, small molecular weight FKBPs from *Manduca sexta* (GA no.: AAF16717) and *Anopheles gambiae* (GA. no.: EAA00155) maintain nearly identical folding patterns when superimposed upon FKBP1 from humans (see Fig. 3). The highly conserved nature of FKBP1 orthologues throughout a wide range of taxonomic groups at both the sequence and higher structural levels suggests that these proteins play a critical role in cellular processes, possibly as chaperones.[39] In addition, it is likely that these proteins also mediate folding in *Manduca sexta* and *Anopheles gambiae*. The partitioning of these structures into groups with seemingly analogous functions may aid in assigning cellular roles to newly identified FKBPs as they are discovered.

FKBP models suggest both gains and losses of motifs throughout evolution

Interestingly, FKBP1 and FKBP2 orthologues in organisms belonging to some of the older phylogenetic branches (e.g. *Methanococcus jannaschii* and *Brugia malayi*) possess additional N- and C-terminal regions of low complexity that younger lineages lack. The absence of these regions in more modern taxa may have resulted from relaxed selection pressure and evolutionary streamlining of the essential components of the protein over time, leading to the loss of these low complexity regions. In this scenario, FKBP11 and FKBP14 from *Homo sapiens*, which contain similar extensions of the N- and C-termini as those FKBPs found in more basal taxa may represent the retention of the ancestral condition.

The presence of several groups of FKBPs, including FKBP1, FKBP2, FKBP3, and FKBP4/5 in the more ancestral lineages indicates an ancient origin for the FKBP motif and suggests several independent duplication events early in evolution. In addition, the structural similarity between FKBPs from distantly related taxa supports the hypothesis that the FKBP region duplicated independently multiple times. In addition, insertion events of various types of domains within FKBP genes may have

taken place in basal phylogenetic branches and have subsequently been conserved throughout evolution.

Docking simulations reveal variable drug-ligand conformations

Despite various single amino acid substitutions among members of the FKBP1 and FKBP2 groups, all of the FKBP1 and FKBP2 orthologues maintain the typical half β-barrel shape characteristic of FKBP domains.[26,40] Docking simulations also suggest that many of the structural elements necessary for the interaction between FKBPs and FK506 remain intact among members of FKBP groups in all organisms examined. Docking models accurately predict the active site for FK506 within FKBP1 in humans, although the docking results place FK506 further inside the binding pocket and rotated the ligand downward compared to the crystal structure (see Fig. 4). Minor variations in the orientation of the drug are also observed among members of the FKBP1 and FKBP2 groups, which may suggest that each protein has a slightly different affinity for FK506.

It is known that human FKBP1, FKBP2 and FKBP3 demonstrate different binding capacities for FK506 (K_d = 0.4, 55, and 160 nM, respectively),[41] with the K_d increasing in relation to the total size of the protein. Although there appear to be only slight structural differences among the active sites themselves, differential affinity of these proteins for FK506 may be attributable in part to the extra domains found within FKBP2 and FKBP3. Additional peptide segments within these proteins, such as those observed in the *Methanococcus jannaschii* FKBP2 appear to affect drug docking, placing the drug outside the previously established active site when compared with other FKBP2s from different species. As reflected in the docking predictions, external helices and other structures may also modulate the interactions through steric hindrance and repulsion near the active site. These additional sequences may also create novel, lower affinity drug binding sites.

## TASSER models provide a first look at FKBP45 and its orthologues

FKBP45 (Group 3, FKBP3-like proteins) from *Bombyx mori* is of particular interest due to its potential role in pre-mRNA splicing.[19] This protein and most of its orthologues appear to be comprised of three major structural regions. Residues Met[1]-Leu[90] corresponds to a tightly folded area of low complexity. Amino acids Asp[91]-Glu[287] consist of alternating E-D and K-R rich repeats ~10–30 amino acids in length, which make up several looping α-helices containing nuclear localization signals.[19] The remaining 114 residues, Lys[288] to Lys[402] correspond to the FKBP domain. The N-terminal region exhibits a unique folding pattern, however, the FKBP motif maintains the same conformation as the archetypal
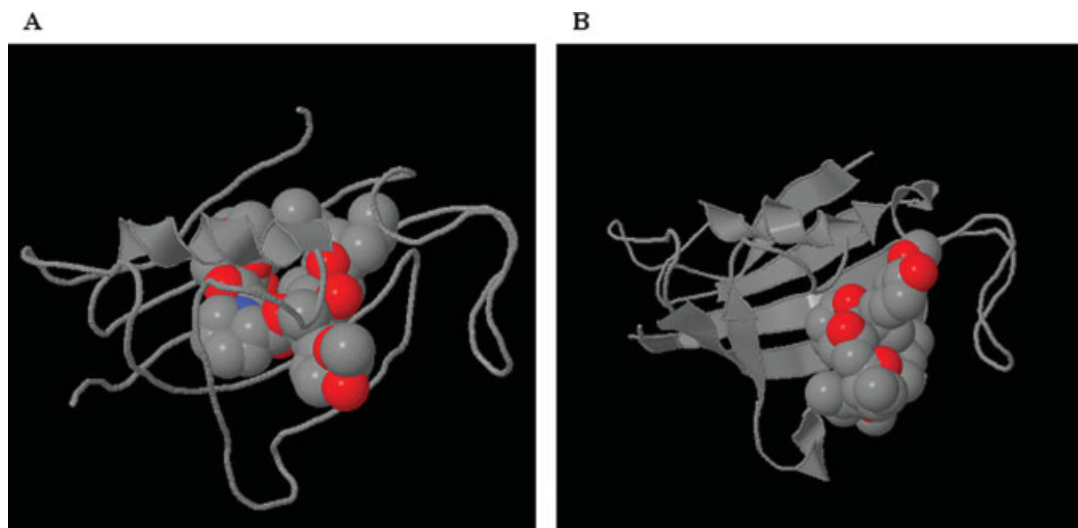
Figure 4

Docking simulations suggest that FKBP orthologues may have differential affinity for FK506. FK506-FKBP interactions were modeled using the ZDOCK server and compared with previously determined FK506-FKBP solution structures. Docking simulations using Homo sapiens *FKBP1 and FK506 correctly predicted the drug active site; however, ZDOCK showed FK506 bound more internally (**A**) within the active site when compared to the solution structure complex (**B**). These models revealed the potential for different orthologues to bind FK506 in slightly different orientations, which may reflect subtle differences in affinity among FKBPs.*

FKBP1 counterpart in humans. Although docking simulations place FK506 outside of the active site [indicated in brackets in Fig. 5(A)] and along the folded alpha helices from Glu[108]-Lys[139] [Fig. 5(A)], the active site of the

FKBP domain within FKBP45 in the silk moth is nearly identical to FKBP1 in humans. Several closely related proteins to FKBP45 in other species bind FK506, including FKBP46 from *Spodoptera frugiperda*,[17] FKBP3 in
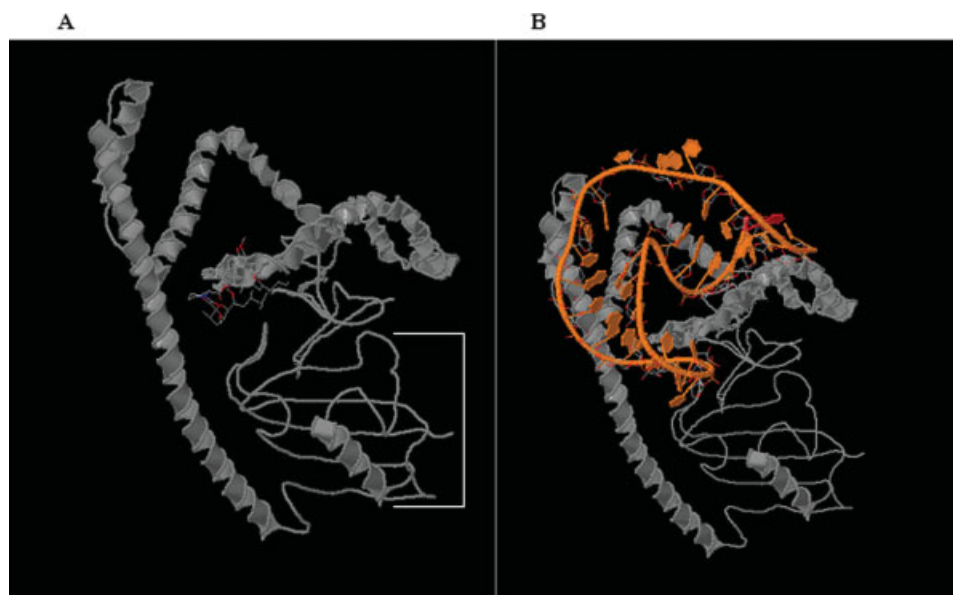
Figure 5

FKBP45 from Bombyx mori *may possess an overlapping active site for both FK506 and RNA. Identification of the potential active site for FK506 (**A**) and a stem-loop RNA (**B**) within* Bombyx mori *FKBP45 indicates that the protein may associate with the drug and RNA in the same region. The characteristic FK506 rapamycin-binding domain is outlined in white brackets. These simulations also suggest that additional regions surrounding the FKBP drug binding pocket may reduce the protein's affinity for FK506 and/or create novel sites for protein-drug interactions.*

humans[10] and the FKBP in *Saccharomyces cerevisiae*,[42] suggesting that FKBP45 also possesses drug-binding ability. It is possible that this additional N-terminal helical region may affect the drug's access to the predicted active site and/or creates a novel drug-binding motif.

Docking experiments, as well as structural superpositions among FKBP45 orthologues also revealed an RNA-binding domain within FKBP45. Previous sequence comparisons between FKBP45 and RNA-binding domains suggested that the FKBP45 RNA-binding region may reside in the N-terminal 225 amino acids.[19] Utilizing the tertiary structures of FKBP45 and an RNA stem-loop (PDB ID: 1AUD), docking simulations placed the active site for stem-loop RNA among four N-terminal helices, Asp^{96}-Val^{105}, Ala^{114}-Lys^{135}, Ala^{141}-Asp^{152} and Lys^{245}-Lys^{261} [Fig. 5(B)]. Moreover, in simulation studies RNA interacts with the same HLH region within all other members of this FKBP group. This region was previously predicted to be the DNA-binding region for FKBP3 in humans[8] and FKBP46 in *Spodoptera frugiperda*.[17] As indicated by the docking simulations, the binding sites of FK506 and RNA overlap and therefore, they may compete for access to the FKBP motif. It is noteworthy that the HLH motif of FKBP45 shares considerable structural similarity with the DNA binding region of human FKBP3, especially within regions that are thought to be of functional importance. Given the high degree of structural similarity between these two proteins, it is possible that FKBP3 is also capable of associating with U1 snRNA.

FKBP3s from different species possess N-terminal domains of low complexity capable of adopting different conformations. Although this may be the result of inaccurate folding predictions due to the lack of comparable structures in the PDB, it is also possible that these regions are not functionally necessary and are not subject to the same level of selection pressure as, for example, the PPIase and HLH domains, both of which have well defined functional roles and maintain consistent shapes through evolution.[8,17,19] The fact that species from early and recent lineages possess FKBP3 orthologues without the N-terminal low complexity domain suggests that gains and losses of this variable region do not strongly affect the function aspect of this protein.

Analysis of multi-FKBP domain proteins

Models of the FKBP4 and FKBP5 members possess the same overall structural arrangement consisting of two FKBP domains and 3–4 pairs of helical TPR motifs. The FKBP domains are rotated ~90° about a 10 residue loop. In general, the folding predictions are nearly identical to the crystal structures of FKBP4 and FKBP5.[30] Yet, unlike the crystal structures, where the TPR motif of FKBP5 is packed more closely to the FKBP domains than in FKBP4,[30] the TPR regions from the predicted FKBP4 and FKBP5 topologies can be superimposed completely.

It has been suggested that the differences in orientation of the TPR motif may be attributed to variations in crystal packing.[30] It is possible that the flexibility in the TPR region contributes to the ability of these proteins to assemble into high molecular weight complexes by way of conformational changes that reduce steric hindrance between multiple protein aggregates.[43]

Based on sequence alignments, FKBP9 and FKBP10 from humans appear to contain four FKBP domains (data not shown); however, the predicted structure reveals only two N-terminal regions that maintain the half β-barrel conformation of the FKBP domain, while the more C-terminal FKBP motifs have lost this typical morphology [Fig. 2(H)]. It is possible that the best templates for these two proteins exhibit structural mismatches in the C-terminal FKBP motif. FKBP5 was used as the template for both of these proteins, and it may be that the C-terminal TPR domain within FKBP5 did not fit the target proteins in these regions. This may also be due to amino acid substitutions within the FKBP domain that have compromised its structure, although no significant differences exist among these domain sequences. Docking simulations using the ZDOCK server indicate that the immunosuppressive drug FK506 binds preferentially to the most C-terminal FKBP domain of both FKBP9 and FKBP10 (data not shown). Although we do not have an explanation, it is interesting that the two FKBP domains lacking the β-barrel conformation bind preferentially to FK506.

CONCLUSIONS

Functional interactions among biological molecules are tightly linked to their three-dimensional structures. The FKBPs represent a unique protein family consisting of several, multi-domain proteins with a variety of cellular roles. An understanding of structural relationships among these proteins is necessary to address questions involving their evolution and assortment of functions. Sequence and topological variations among these proteins resulting in different affinities for ligands may allow for modulation and diversity of function.

REFERENCES

1. Harding MW, Galat A, Uehling DE, Schrieber SL. A receptor for the immunosuppressant FK506 is a cis-trans peptidyl-prolyl isomerase. Nature 1989;341:758–760.
2. Standaert RF, Galat A, Verdine GL, Schreiber SL. Molecular cloning and overexpression of the human FK506-binding protein FKBP. Nature 1990;346:671–674.
3. Galat A. Peptidylproline cis-trans isomerases: immunophilins. Eur J Biochem 1993;216:689–707.
4. Kay JE. Structure-function relationships in the FK506-binding protein (FKBP) family of peptidylprolyl *cis-trans isomerases*. Biochem J 1996;314:361–385.
5. Schiene C, Fisher G. Enzymes that catalyze the restructuring of proteins. Curr Opin Struct Biol 2000;10:40–45.

6. Davies TH, Sanchez ER. FKBP52. Int J Biochem Cell Biol 2005; 37:42–47.

7. Rulten SL, Kinloch RA, Tateossian H, Robinson C, Gettins L, Kay JE. The human FK506-binding proteins: characterization of human FKBP19. Mamm Genome 2006;17:322–331.

8. Riviere S, Menez A, Galat A. On the localization of FKBP25 in T-lymphocytes. FEBS Lett 1993;315:247–251.

9. Nakamura T, Yabe D, Kanazawa N, Tashiro K, Sasayama S, Honjo T. Molecular cloning, characterization, and chromosomal localization of FKBP23, a novel FK506-binding protein with Ca^{2+}-binding ability. Genomics 1998;54:89–98.

10. Jin YJ, Burakoff SJ, Bierer BE. Molecular cloning of a 25-kDa high affinity rapamycin binding protein. FKBP25. J Biol Chem 1992;267: 10942–10945.

11. Jin YJ, Albers MW, Lanei WS, Beirer BE, Schreiber SL, Burakoff SJ. Molecular cloning of a membrane-associated human FK506- and rapamycin-binding protein. FKBP-13 (rotamase/T-cefl activation/mast cell). Immunology 1991;88:6677–6681.

12. Liu J, Farmer JD, Jr, Lane WS, Friedman J, Weissman I, Schreiber SL. Calcineurin is a common target of cyclophilin-cyclosporin A and FKBP-FK506 complexes. Cell 1991;66:807–815.

13. Rao A, Luo C, Hogan PG. Transcription factors of the NF-AT family: regulation and function. Annu Rev Immunol 1997;15: 707–747.

14. Li TK, Baksh S, Cristillo AD, Bierer BE. Calcium- and FK506-independent interaction between the immunophilin FKBP51 and calcineurin. J Cell Biochem 2002;84:460–471.

15. Marks AR. Cellular functions of immunophillins. Physiol Rev 1996; 76:631–649.

16. Morita K, Kitayama T, Kitayama S, Dohi T. Cyclic ADP-ribose requires FK506-binding protein to regulate intracellular Ca2+ dynamics and catecholamine release in acetylcholine-stimulated bovine adrenal chromaffin cells. J Pharmacol Sci 2006;101:40–51.

17. Alnemri ES, Fernandes-Alnemri T, Pomerenke K, Robertson NM, Dudley K, DuBois GC, Litwack G. FKBP46, a novel Sf9 insect cell nuclear immunophilin that forms a protein-kinase complex. J Biol Chem 1994;269:30828–30834.

18. Xiaoa H, Jackson V, Leia M. The FK506-binding protein. Fpr4, is an acidic histone chaperone. FEBS Lett 2006;580:4357–4364.

19. Somarelli JA, Coll JC, Velandia A, Martinez L, Herrera RJ. Characterization of immunophilins in the silkmoth *Bombyx mori*. Arch Insect Biochem Physiol 2007;65:195–209.

20. Goel M, Garcia R, Estacion M, Schilling WP. Regulation of *Drosophila* TRPL channels by immunophilin FKBP59. J Biol Chem 2001;276:38762–38773.

21. Kurek I, Dulberger R, Azem A, Tzvi BB, Sudhakar D, Christou P, Breiman A. Deletion of the C-terminal 138 amino acids of the wheat FKBP73 abrogates calmodulin binding, dimerization and male fertility in transgenic rice. Plant Mol Biol 2002;48:369–381.

22. Sinars CR, Cheung-Flynn J, Rimerman RA, Scammell JG, Smith DF, Clardy J. Structure of the large FK506-binding protein FKBP51, an Hsp90-binding protein and a component of steroid receptor complexes. PNAS 2003;100:868–873.

23. Tranguch S, Cheung-Flynn J, Daikoku T, Prapapanich V, Cox MB, Xie H, Wang H, Das SK, Smith DF, Dey SK. Cochaperone immunophilin FKBP52 is critical to uterine receptivity for embryo implantation. Proc Natl Acad Sci USA 2005;102:14326–14331.

24. Edlich F, Weiwad M, Erdmann F, Fanghanel J, Jarczowski F, Rahfeld JU, Fischer G. Bcl-2 regulator FKBP38 is activated by Ca2+/calmodulin. EMBO J 2005;24:2688–2699.

25. Wang HQ, Nakaya Y, Du Z, Yamane T, Shirane M, Kudo T, Takeda M, Takebayashi K, Noda Y, Nakayama KI, Nishimura M. Interaction of presenilins with FKBP38 promotes apoptosis by reducing mitochondrial Bcl-2. Hum Mol Genet 2005;14:1889–1902.

26. Maestre-Martinez M, Edlich F, Jarczowski F, Weiwad M, Fischer G, Lucke C. Solution structure of the FK506-binding domain of human FKBP38. J Biomol NMR 2006;34:197–202.

27. Wilson KP, Yamashita MM, Sintchak MD, Rotstein SH, Murcko MA, Boger J, Thomson JA, Fitzgibbon MJ, Black JR, Navia MA. Comparative X-ray structures of the major binding protein for the immunosuppressant FK506 (tacrolimus) in unliganded form and in complex with FK506 and rapamycin. Acta Cryst D 1995;51:511–521.

28. Van Duyne GD, Standaert RF, Karplus PA, Schreiber SL, Clardy J. Atomic structure of FKBP-FK506, an immunophilin-immunosuppressant complex. Science 1991;252:839–842.

29. Schultz LW, Clardy J. Chemical inducers of dimerization: the atomic structure of FKBP12-FK1012A-FKBP12. Bioorg Med Chem Lett 1998;8:1–6.

30. Wu B, Li P, Liu Y, Lou Z, Ding Y, Shu C, Ye S, Bartlam M, Shen B, Rao Z. 3D structure of human FK506-binding protein 52: Implications for the assembly of the glucocorticoid receptor/Hsp90/immunophilin heterocomplex. PNAS 2004;101:8348–8353.

31. Zhang Y, Arakaki AK, Skolnick J. TASSER: an automated method for the prediction of protein tertiary structures in CASP6. Proteins 2005;7:91–98.

32. Skolnick J, Kihara D, Zhang Y. Development and large scale benchmark testing of the PROSPECTOR_3 threading algorithm. Proteins 2004;56:502–518.

33. Zhang Y, Skolnick J. SPICKER: a clustering approach to identify near-native protein folds. J Comput Chem 2004;25:865–871.

34. Zhang Y, Skolnick J. Automated structure prediction of weakly homologous proteins on a genomic scale. Proc Natl Acad Sci USA 2004;101:7594–7599.

35. Gille C, Frommel C. STRAP: editor for structural alignments of proteins. Bioinformatics 2001;17:377–378.

36. Bjellqvist B, Hughes GJ, Pasquali C, Paquet N, Ravier F, Sanchez ,J-Ch, Frutiger S, Hochstrasser DF. The focusing positions of polypeptides in immobilized pH gradients can be predicted from their amino acid sequences. Electrophoresis 1993;14:1023–1031.

37. Gasteiger E, Hoogland C, Gattiker A, Duvaud S, Wilkins MR, Appel RD, Bairoch A. Protein identification and analysis tools on the ExPASy server. In: John MW, editor. The proteomics protocols handbook. Herts, UK: Humana Press; 2005; pp 571–607.

38. Suzuki R, Nagata K, Yumoto F, Kawakami M, Nemoto N, Furutani M, Adachi K, Maruyama T, Tanokura M. Three-dimensional solution structure of an archaeal FKBP with a dual function of peptidyl prolyl cis-trans isomerase and chaperone-like activities. J Mol Biol 2003;328:1149–1160.

39. Somarelli JA, Herrera RJ. Evolution of the 12kDa FK506-binding protein gene. Biol Cell 2007;99:311–321.

40. Van Duyne GD, Standaert RF, Schreiber SL, Clardy J. Atomic structure of the rapamycin human immunophilin Fkbp-12 complex. J Am Chem Soc 1991;113:7433–7434.

41. Braun W, Kallen J, Mikol V, Walkinshaw MD, Wuthrich K. Three-dimensional structure and actions of immunosuppressants and their immunophilins. FASEB J 1995;9:63–72.

42. Manning-Krieg UC, Henriquez R, Cammas F, Graff P, GavCriaux S, Movva NR. Purification of FKBP-70, a novel immunophilin from *Saccharomyces cerevisiae*, and cloning of its structural gene, FPR3. FEBS Lett 1994;352:98–103.

43. Stanley WA, Pursiainen NV, Garman EF, Juffer AH, Wilmanns M, Kursula P. A previously unobserved conformation for the human Pex5p receptor suggests roles for intrinsic flexibility and rigid domain motions in ligand binding. BMC Struct Biol 2007;7:1472–6807.